Iron, and manganese doped SO_4^{2-}/ZrO_2–TiO_2 mixed oxide catalysts: studies on acidity and benzene isopropylation activity

D. Das[a], H.K. Mishra[a], A.K. Dalai[a,*], and K.M. Parida[a,b]

[a]*Catalysis and Chemical Reaction Engineering Laboratories, Department of Chemical Engineering, University of Saskatchewan, Saskatoon SK, Canada*

[b]*Environment Management and Inorganic Chemicals Division, Regional Research Laboratory (CSIR), Bhubaneswar 751 013, India*

Received 12 August 2003; accepted 9 January 2004

Sulfated zirconia–titania and its transition metal doped compositions with 1.5 wt% iron, and 0.5 wt% manganese were prepared and characterized for surface acidity, and activity towards benzene alkylation. Acidity measurement of the 600 °C calcined samples showed that upon doping with Mn, the protonic acid strength of the material increased, whereas iron doping decreased the strength of surface protons and followed the order Mn-SO_4^{2-}/ZrO_2–TiO_2 > SO_4^{2-}/ZrO_2–TiO_2 > Fe-SO_4^{2-}/ZrO_2–TiO_2. Samples calcined at 110 and 600 °C were XRD amorphous. However, on calcination at 800 °C these samples showed crystalline phases characteristic of $ZrTiO_4$. The Mn doped catalyst also showed highest activity and improved catalyst stability towards isopropylation of benzene. A good correlation between surface acidity and isopropylation activity was obtained. Increase in acidity in case of Mn doped sample was attributed to the increased stability of the surface sulfate groups.

KEY WORDS: sulfated zirconia–titania; metal doping; surface acidity; isopropylation.

1. Introduction

Sulfated zirconia has attracted much attention of researchers [1–6] due to its high acidity and ability to catalyze *n*-butane isomerization at low temperature. But, its fast deactivation and small lifetime for hydrocarbon isomerization reactions has prevented its direct use in commercial processes. The recent research on sulfated zirconia is mainly concentrated in understanding the mechanism of deactivation and developing a more stable catalyst with longer lifetime through impregnation of different active components on its surfaces. The presence of noble metal crystallites in sulfated zirconia catalyst formulation enhances their activity and/or stability [7–9], but their mode of accomplishing this effect has not been well established. Since, platinum and other noble metals are expensive, approaches have been made to use other metals maintaining the equivalent activity and stability. A new class of solid acid catalyst with iron and/or manganese promoted sulfated zirconia has been reported to have *n*-butane isomerization activity two to three orders of magnitude more than that of sulfated zirconia [10]. But, the actual cause of this huge increment in isomerization activity upon doping with manganese and/or iron is still not clear.

In addition to ZrO_2, many other metal oxides such as Fe_2O_3, TiO_2 etc. when promoted with sulfate ions, develop strong acidity and have been investigated for several acid catalyzed reactions [4,11]. Though, the literature on single metal oxides as acid catalysts is abundant, only a few reports are available on the use of mixed/complex metal oxides as acid catalysts, excepting silica–alumina. Mixed oxides often show enhanced acidity in comparison to the respective single metal oxides [12]. Mixing of two oxides may modulate the properties of the component oxides or generate new active sites. The acidity of the mixed oxides is believed to be resulting from the excess of negative or positive charges caused by the bridged hetero metal–oxygen bonds (M—O—M′) [12]. In a mixed oxide containing two different metals M and M′ the degree of M—O—M′ bond depends upon the degree of mixing of M and M′. In fact, the acidity, which is one of the most important factors to determine the catalytic activity, depends upon the mixing of two metal components through oxygen, namely the homogeneity of the mixed oxide. In our earlier communication, it was reported ZrO_2–TiO_2 mixed oxides containing 60 mol% Zr imparted highest surface area with highest acidity [13]. This material when sulfated also showed highest activity towards 2-propanol dehydration. Indeed, ZrO_2–TiO_2 mixed oxide possesses some interesting catalytic properties. They are active for cyclohexene oxide isomerization to allyl alcohols [14], dehydrogenation of ethyl benzene to styrene [15,16], and dehydrocyclization of C_6–C_8 *n*-parafins to aromatics [17]. Moreover, they have also been tested as a support for platinum in the reforming of *n*-hexane, and the selectivity of the sum of the cyclic and aromatization reactions over ZrO_2–TiO_2 catalyst with a 50% content of each oxide, was found to be higher than that of a commercial catalyst [18].

* To whom correspondence should be addressed.
E-mail: dalai@engr.usask.ca

1011-372X/04/0300–0185/0 © 2004 Plenum Publishing Corporation

In our earlier communication, we reported the isopropylation of benzene to cumene using 2-propanol as the alkylating agent over sulfated ZrO_2–TiO_2 mixed oxide catalysts [19]. Though, this catalyst had very good activity, the fast deactivation of alkylation sites was the major concern. In this communication, the physicochemical and surface properties of pure and Mn, and Fe doped sulfated ZrO_2–TiO_2 catalysts have been investigated. A detailed study was performed to understand acidity changes upon doping with Mn and Fe. Furthermore, these characteristics were correlated to their isopropylation activities.

2. Experimental

2.1. Material preparation

ZrO_2–TiO_2 mixed oxide was prepared by co-precipitation method taking $ZrOCl_2$. $8H_2O$ (Merck, 99%), and $TiCl_4$ (Spectrochem, AR) as the precursor materials and sodiumdodecylsulfate as templating agent. The mixture of acetyl acetone (BDH, LR), ethyl alcohol and ammonium hydroxide (both from Merck) was stirred in a stainless steel bomb reactor for about 10 min, and to this required amount of sodiumdodecylsulfate (Sdfines Chemicals, 99%) was added and stirred for another 10 min to get a clear solution. To this, required amount of premixed $ZrOCl_2$ and $TiCl_4$ solution containing 60 mol% zirconium and 40 mol% titanium was poured in a lot under vigorous stirring condition, and the mixture was stirred for another 20 min. Then the basic colloidal solution was charged inside a reactor for hydrothermal reaction at 110 °C for 6 h (not stirred). The precipitate was filtered, washed with deionized water until it was freed from chloride ions (negative $AgNO_3$ test) and dispersed thrice in distilled ethanol. It was then dried, initially at 60 °C for 5 h and then at 110 °C overnight. The dried gels were loaded with 10 wt% sulfate using 0.25 M H_2SO_4 solution and dried overnight at 110 °C in an oven. For preparing Fe, and Mn doped samples, the 110 °C dried powdered sulfated sample was suspended in required amounts of 0.25 M precursor salt (in their nitrate forms, BDH, AR) solutions to maintain Fe, and Mn contents of 1.5 and 0.5 wt%, respectively. The solution was evaporated to dryness under stirring conditions and dried at 110 °C for overnight. These dried materials were calcined at different temperatures (600 and 800 °C) for 3 h to prepare SO_4^{2-}/ZrO_2–TiO_2, Fe–SO_4^{2-}/ZrO_2–TiO_2 and Mn–SO_4^{2-}/ZrO_2–TiO_2.

2.2. Characterization

2.2.1. X-ray powder diffraction

The crystallographic phase identification of the 600 and 800 °C calcined samples was carried out in an X-ray powder diffractometer (Rigaku, Tokyo, Japan) using FeKα radiation and fitted with graphite monochromator. The samples were scanned in the range of $2\theta = 4°$–60° to record the spectra.

2.2.2. Nitrogen adsorption–desorption

The BET surface area, total pore volume and average pore diameter were analyzed by multipoint N_2 adsorption/desorption method at liquid N_2 temperature (77 K) with a Michromeritics (ASAP 2000) instrument. Prior to analyses, all samples were degassed at 200 °C and 10^{-4} Torr pressure to evacuate the physisorbed moisture.

2.2.3. NH_3 temperature programmed desorption (TPD)

The NH_3-TPD of both undoped and metal doped samples was carried out in a CHEM BET-3000 (Quanta chrome, USA) instrument. About 0.1 g of powdered sample was taken inside a quartz "U" tube and degassed at 400 °C for 1 h with ultrapure helium gas flow. The sample was than cooled to 30 °C and the gas flow was changed to NH_3 for 30 min. The NH_3 adsorbed sample was then purged with He flow for another 30 min at the same temperature to remove any weakly adsorbed NH_3 on the catalyst surface. It was then heated up under helium flow (35 mL/min) at a heating rate of 10 °C/min to record the spectra.

2.2.4. ^1H MAS NMR

The ^{1}H MAS NMR spectra of the catalysts were recorded using a Bruker Advanced DRX 360WB spectrometer (Bruker BioSpin Ltd.). The magic angle spinning (MAS) frequency of 5 kHz was used during the spectral acquisition. The instrument was operated at a resonance frequency of 360.13 MHz. Before carrying out the NMR analysis, all the samples were heated at 200 °C for 2 h and carried in a properly sealed sample tube.

2.2.5. Temperature programmed reduction (TPR)

The TPR spectra of the catalysts were recorded by using a CHEM BET-3000 (Quanta chrome, USA) instrument. In a typical experiment, about 0.1 g of catalyst was placed in between two quartz wool plugs in a quartz U-tube and heated at 200 °C for 1 h under ultra-pure He gas flow. Then, the U-tube was cooled down to room temperature. The gas flow was then changed to 3%H_2 in N_2 and the TPR experiments were performed by heating the catalyst under helium flow (Rate-35 mL/min) at a heating rate of 10 °C/min.

2.3. Catalytic activity test

The catalytic activities of the samples were tested for isopropylation of benzene using isopropanol. In a typical experiment, 0.5 g of powdered catalyst was loaded between two quartz wool plugs at the center of a down flow stainless steel micro reactor (8 mm id).

Before the catalytic activity test, the catalyst was pretreated at 400 °C for 1 h under nitrogen flow (30 mL/min) and then cooled down to the reaction temperature. The pretreatment was carried out to get rid of adsorbed species from the catalyst surface, if present. N_2 was used as both pretreatment and carrier gas and the flow rate was maintained at 30 mL/min by a mass flow meter (Matheson). Mixture of benzene (BDH, 99.5 % pure) and isopropanol (BDH, 99.5% pure) was used as the feed. Required amount of the liquid mixture was pumped by a programmable syringe pump (Genie, Kent Scientific Corporation, Model-YA-12) and was fed from the top of the reactor after being vaporized by a pre-heater maintained at about 120 °C. The catalytic activity was tested at atmospheric pressure. The products were trapped in a condenser at the reactor outlet and analyzed in FID mode after each 1 h by a VARIAN GC (model-3400) using 30 m long DBPS-1 capillary column coated with 100% methylsiloxane as a stationary phase. The gaseous products were collected and analyzed by HP GC (model-5880) in FID mode fitted with Chromosorb packed column.

The chemical reaction between benzene and isopropanol over sulfated and transition metal doped ZrO_2–TiO_2 mixed oxide catalysts generated several products. The two reactions involved are dehydration of isopropanol to prorene and alkylation of benzene with propene to give a range of alkylated products. These two major reactions are often accompanied by several others such as transalkylation, disproportionation, etc. The present work revealed only the presence of propene, cumene, di- and tri-isopropylbenzenes in the product stream. Based on these observations and earlier work [19], the overall chemical reaction between benzene and isopropanol can be presented as follows.

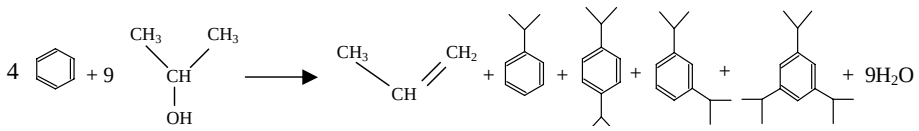

(1)

Each set of experiment was done three times and the error was within ±6%. To minimize error in the reported data, the average of results from three runs was taken. Mass balance for each run was always >97%. The conversions, both with respect to benzene and isopropanol, were calculated using the equation:

$$\% X = \frac{C_i - C_p}{C_i} \times 100 \quad (2)$$

where

X = conversion,

C_i = moles of benzene/isopropanol injected per hour per gram of catalyst,

C_p = moles of benzene/isopropanol present in product stream per hour per gram of catalyst.

The product selectivity was calculated by taking the total number of moles of product formed following the equation:

$$\% S_i = \frac{P_i}{P_t} \times 100 \quad (3)$$

where

S_i = selectivity of ith component,

P_i = moles of the ith product component formed per hour per gram of catalyst,

P_t = total number of moles of product formed per hour per gram of catalyst.

3. Results and discussion

3.1. X-ray diffraction

When the active metals are doped over catalyst/support, their distribution/dispersion may affect the overall catalytic activity. After calcination at high temperature, the dispersed metals may come closer to form big crystallites and decrease the performance of catalyst. To know the effect in case of manganese and iron doped catalysts, X-ray diffraction of both undoped and doped sulfated ZrO_2–TiO_2 mixed oxides calcined at 800 °C was carried out and the patterns are shown in figure 1. All the catalysts developed $ZrTiO_4$ as a single phase. In our earlier communications, it was reported that sulfated ZrO_2–TiO_2 mixed oxide when calcined at 800 °C, had developed only single $ZrTiO_4$ phase, though the ZrO_2 content in the mixed oxide was 60 mol% [13,19]. The iron, and manganese doped catalysts did not show any XRD peak corresponding to either of the doped metal oxide crystallites. This could be due to the presence of metals in well-dispersed state on ZrO_2–TiO_2 mixed oxide surface. The 110 and 600 °C calcined catalysts were found XRD amorphous (spectra not given).

3.2. Surface area, pore volume and pore size distribution

The activity of a solid catalyst is dependent on its several characteristics such as available surface are, pore volume and pore diameter, amount of active sites available for interaction, interaction of active phase with catalyst, etc. In this present case the sulfated ZrO_2–TiO_2 mixed oxide was doped with iron and manganese and the presence of these metals may modify the surface

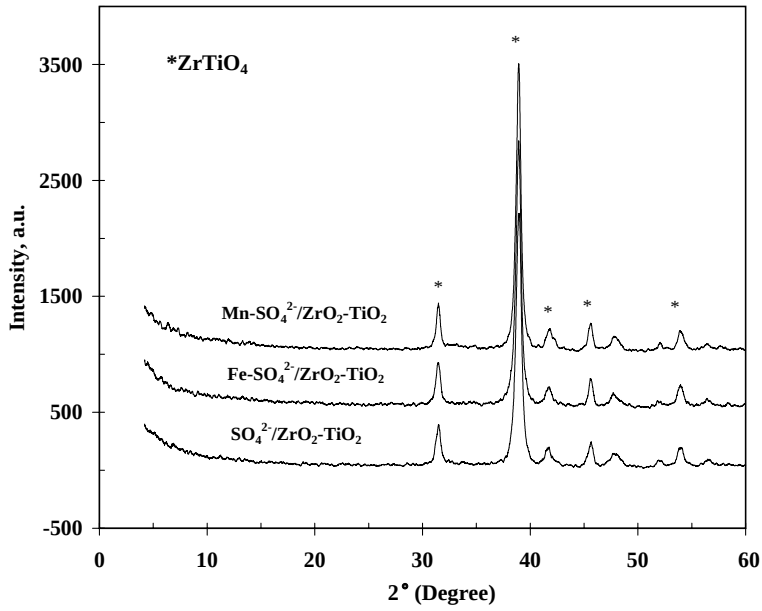

Figure 1. X-ray diffraction patterns of undoped, and iron and manganese doped SO_4^{2-}/ZrO_2–TiO_2 mixed oxide catalysts calcined at 800 °C.

Table 1
Surface area, total pore volume and average pore diameter of undoped and iron and manganese doped SO_4^{2-}/ZrO_2–TiO_2 catalysts calcined at 600 °C

Catalyst	BET surface area (m^2/g)	Average pore diameter (Å)	Total pore volume (cc/g)
SO_4^{2-}/ZrO_2–TiO_2	137	137.7	0.47
Mn–SO_4^{2-}/ZrO_2–TiO_2	50	219.9	0.37
Fe–SO_4^{2-}/ZrO_2–TiO_2	107	131.8	0.35

and pore structures of the parent material. Furthermore, this may change other properties such as surface acidity and catalytic activity, which will be discussed in the following sections. Table 1 shows the BET surface area, total pore volume and average pore diameter of undoped and iron and manganese doped SO_4^{2-}/ZrO_2–TiO_2 catalysts calcined at 600 °C. It is evident from the table that for iron doped catalyst, both surface area and pore volume were decreased. At the same time there was a slight decrease in average pore diameter. This could be due to the pore mouth blockage by the Fe particles. But, for Mn promoted catalyst decrease in surface area (approximately 63%) was observed followed by very sharp increase in average pore diameter (approximately 60%). This shows that, drastic modifications of pore structures take place when sulfated ZrO_2–TiO_2 mixed oxide gels are doped with transition metals, and further, the effect probably depends upon the individual metal characteristics. The decrease in surface area and corresponding increase in average pore diameter may be due to the collapse of considerably narrow pores to form broad pores in presence of Mn. This effect is not observed when the same material is promoted with iron.

3.3. NH_3 temperature programmed desorption

Figure 2(a) depicts the NH_3 TPD patterns of both pure, and iron and manganese doped sulfated ZrO_2–TiO_2 mixed oxide catalysts. As evident from the figure, the distributions of the acid sites remained same irrespective of whether there was any metal ion doping or not. Each of the profiles showed two peaks corresponding to desorption of NH_3 bound to the oxide surface. The peak below 500 °C is broad and represents the acidic center of medium strength. The broad peak started slightly above 100 °C for Fe doped catalyst as that of the undoped catalyst. But, the same peak was shifted about 100 °C higher when the catalyst was doped with Mn. This broad desorption peak is believed to be merging from four different component peaks, which is clearly visible in figure 2(b). Peak L_1 is assigned to NH_3 released from weak Lewis acid sites such as coordinately unsaturated zirconium and titanium ions [20,21]. Peak L_2 is assigned to the release of NH_3 H-bonded to strong Bronsted acid sites bound NH_4^+ species [20,21]. Peak L_3 is designated to desorption of NH_3 coordinated to NH_3 strongly bonded to strong Lewis acid sites [21]. The peak B is assigned to the NH_3 desorbed from Bronsted acid sites [21].

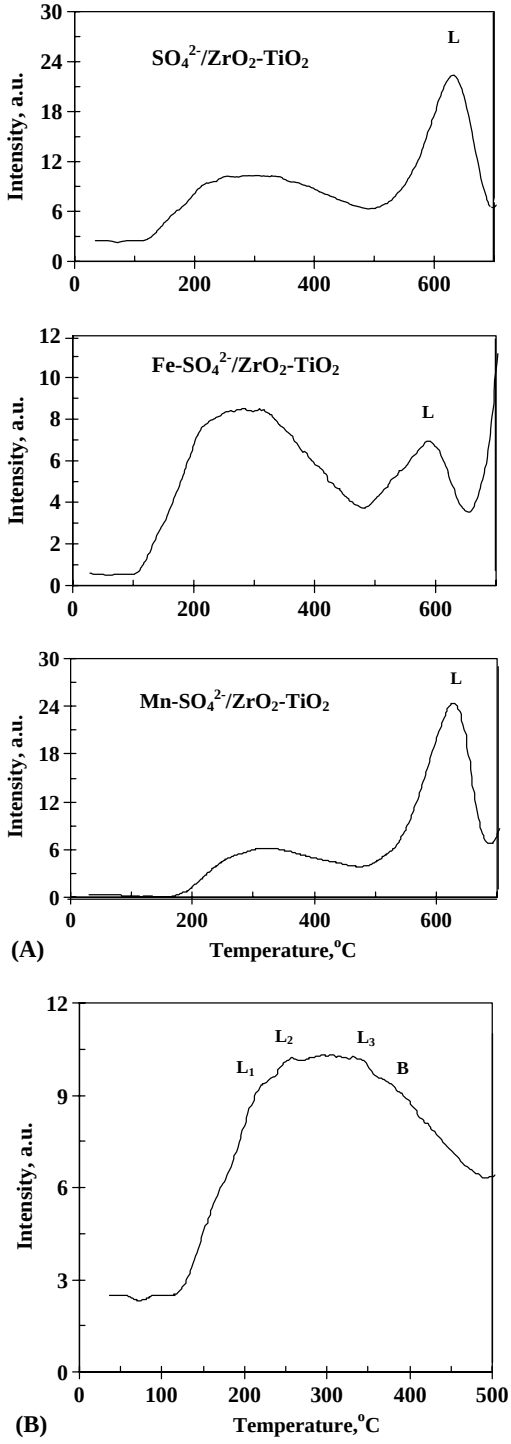

Figure 2. (A) NH_3 TPD profiles of undoped, and iron and manganese doped SO_4^{2-}/ZrO_2–TiO_2(S) mixed oxide catalysts calcined at 600 °C. (B). Distribution of acid sites in NH_3 TPD profile (low temperature) for undoped SO_4^{2-}/ZrO_2–TiO_2(S) mixed oxide catalysts calcined at 600 °C.

Considerably narrow desorption peak at ~600 °C corresponds to NH_3 released from strong acidic centers (Peak L, figure 2(a)). This high temperature desorption peak appeared at slightly higher temperature upon Mn doping than the undoped catalyst (profile for Mn–SO_4^{2-}/ZrO_2–TiO_2, figure 2(a)). On the other hand, for Fe doped catalyst, desorption took place at lower temperature, i.e., at ~570 °C (profile for Fe–SO_4^{2-}/ZrO_2–TiO_2), even lower than that of the undoped catalyst. Furthermore, the peak intensity corresponding to high temperature ammonia desorption was higher for Mn doped catalyst than that of the undoped and iron doped catalyst. These results showed that Fe doping over sulfated ZrO_2–TiO_2 mixed oxide catalyst decreased the number and strength of the stronger acid sites, but upon Mn doping these properties of the catalyst enhanced.

3.4. ^1H MAS NMR

Owing to the high electronegativity of both Zr^{+4} and Ti^{+4} ions in sulfated ZrO_2–TiO_2 mixed oxides, the surface OH groups should develop high protonic acidity. The ^1H chemical shifts have been used by several workers to assign and correlate the acid strengths of surface OH groups [22–24]. Reimer *et al.* [25] studied the ^1H MAS NMR of pure and sulfated ZrO_2. For pure ZrO_2 they found two signals: one intense signal at 3.86 ppm and the other, a comparatively weak peak at 1.60 ppm. The equivalent chemical shifts were also observed by Mastikhin *et al.* [23]. After sulfation the strong signal shifted to 5.85 ppm and this downfield shift was attributed to the increase in acid strength of the surface OH protons. In our case for SO_4^{2-}/ZrO_2–TiO_2 calcined at 600 °C (figure 3(A)), the ^1H MAS NMR spectra showed a single and very intense peak at 5.4 ppm with a small shoulder at 2.08 ppm. The shoulder may be arising due to a very small number of hydrogen atoms. The same type of observation was also made by Semmer *et al.* [26] for sulfated ZrO_2 in which the intense peak appeared at 5.8 ± 0.2 ppm and a small

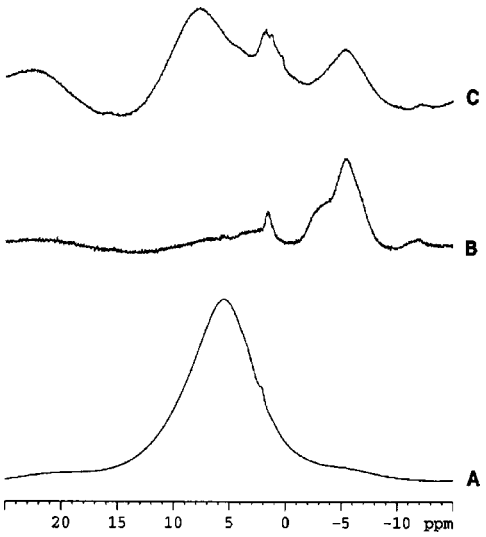

Figure 3. ^1H MAS NMR spectra of undoped, and iron and manganese doped SO_4^{2-}/ZrO_2–TiO_2(S) mixed oxide catalysts calcined at 600 °C. Profile A, B, and C represent SO_4^{2-}/ZrO_2–TiO_2(S), Fe–SO_4^{2-}/ZrO_2–TiO_2(S) and Mn–SO_4^{2-}/ZrO_2–TiO_2(S), respectively.

one at 1.4 ± 0.2 ppm. For Mn doped catalyst, the strong peak shifted towards downfield to 7.62 ppm and the low intense peak that was present in the form of a shoulder in case of SO_4^{2-}/ZrO_2–TiO_2, splitted into a doublet at 1.77 and 1.30 ppm (figure 3(C)). About 2.2 ppm downfield shift of the strong peak after Mn doping confirms the enhancement in the protonic acid strength of this material relative to the undoped catalyst. Further, in addition to the above signals, another signal was observed at −5.35 ppm, which was absent in case of SO_4^{2-}/ZrO_2–TiO_2. On the other hand, the strong peak is totally absent for Fe–SO_4^{2-}/ZrO_2–TiO_2, which indicates the decrease in acidity upon Fe doping. But, the doublet present in case of Mn–SO_4^{2-}/ZrO_2–TiO_2 appeared as a singlet at 1.56 ppm and this chemical shift seems to be the average of that of the doublet. Furthermore, the far upfield signal moved a little more upfield to −5.52 ppm upon Fe doping with a shoulder at about −3.0 ppm.

From the above observations and the previous reports it may be concluded that the Mn doped catalyst contains protons, whose acidity is much stronger than both undoped and iron doped catalyst. The Fe doped catalyst contains the weakest acidic protons among the three catalysts. The enhancement of acidity is attributed to the increase in stability of surface sulfate groups upon Mn doping. To confirm that Mn doping stabilized the surface sulfate, TPR analyses were carried out and the results are discussed below.

3.5. Temperature programmed reduction

From the above two sections it is clear that there is an increase in surface acidity for Mn doped catalyst; but the reason is not very clear. Since the metal oxides/mixed oxides attain high acidity upon sulfation, the sulfate groups on oxide surface are the determining factors for their acidity. To explore this situation, TPR experiments of undoped, and Mn and Fe doped SO_4^{2-}/ZrO_2–TiO_2 catalysts, calcined at 600 °C, were carried out and the profiles are shown in figure 4. The undoped catalyst showed a large reduction peak at 730 °C. This peak was attributed to the reduction of surface sulfate groups. Xu and Sachtler [27] observed the surface sulfate reduction peak at 675 °C for sulfated ZrO_2. Ebitani *et al.* [28] reported the sulfate reduction peak at about 527 °C for Pt-sulfated ZrO_2 catalyst. The same type of observations was also made by other workers [9,29,30]. But, in the present case the appearance of sulfate decomposition peak at higher temperature is attributed to the higher stability of the surface sulfate groups on ZrO_2–TiO_2 surface than on ZrO_2 surface. This result is also in accordance with our previous observations that the higher stability of sulfate groups was obtained over ZrO_2–TiO_2 surface [13]. A close look into figure 4 seems that the sulfate reduction peak is not a single peak, rather, it emerges from the combination of two peaks; one broad peak whose on set starts from

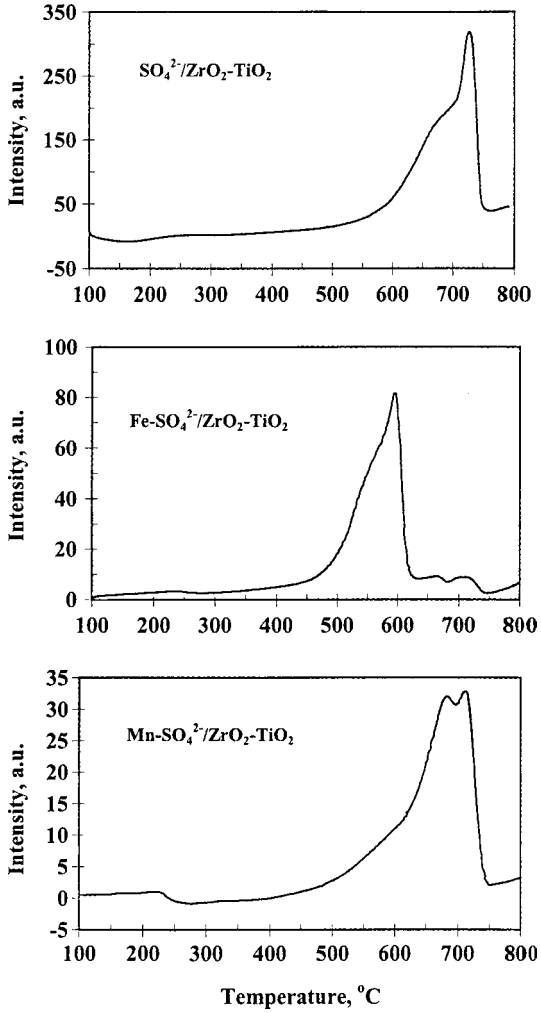

Figure 4. TPR profiles of undoped, and iron and manganese doped SO_4^{2-}/ZrO_2–TiO_2(S) catalysts calcined at 600 °C.

~300 °C with peak maximum ~675 °C and another very sharp peak with peak maximum at ~730 °C. Therefore, it is apparent that there are two types of sulfate groups present on the catalyst surface. One type is comparatively less stable, which is reduced in hydrogen atmosphere at lower temperatures (represented by the broad peak in figure 4) and the second type, being more stable, is reduced at higher temperature (represented by the sharp peak). For metal doped catalysts, the sulfate reduction peaks were observed at relatively lower temperatures, which showed an enhancement of sulfate reduction in presence of metal ions. This observation is in well agreement with those reported by earlier workers [9,28,29], where they observed that Pt metal facilitated sulfate reduction over ZrO_2 surface. Our prediction of the presence of two types of sulfate groups in case of undoped catalyst can be clearly observed from the TPR profiles of Fe and Mn promoted catalysts (figure 4), respectively, which show the presence of two distinct sulfate reduction peaks.

For the Fe promoted catalyst, the high temperature reduction peak was observed at ~580 °C and the low temperature reduction peak (which corresponds to the reduction of less stable surface sulfate species, as we predicted) at ~530 °C. The presence of two peaks can be clearly seen in this case and that in case of Mn promoted catalyst appears like a doublet.

When the decrease in sulfate reduction temperature of Fe and Mn doped catalysts was compared with undoped catalyst, it was observed that in case of Fe, the reduction temperature for both the peaks decreased parallelly at about 150 °C. On the other hand, the high temperature sulfate reduction peak in case of Mn doped sample appeared at the same temperature as that of the undoped catalyst. Also, the low temperature reduction peak remained almost unchanged and they appeared like a doublet. It should be noted here that the Mn loading was 0.5 wt%, whereas Fe loading was 1.5 wt%. So, the question may be raised that the iron loading was much higher than that of manganese and higher iron content decreased the sulfate reduction temperature. To answer this, the TPR of 1.5 wt% manganese doped catalyst was carried out, which showed no change in the sulfate reduction temperature. From the above discussions it is suggested that the surface sulfate groups are less stable in presence of Fe over ZrO_2–TiO_2 surface. On the other hand, the presence of Mn does not affect the reduction of sulfate. From the above observations, it may be concluded that Mn doping adds more stability to the surface sulfate groups over ZrO_2–TiO_2 surface. This could be the reason for the enhancement of acidity in case of Mn doped catalyst, as indicated by ^{1}H NMR and higher catalytic activity for isopropylation of benzene. So the enhancement of acidity could be attributed to the more stability of surface sulfate groups in presence of Mn. But, this acidity increase could not be well observed by NH_3 TPD, as being a strong base, NH_3 adsorbed on all acid sites and the same types of profiles were observed for all the catalysts. The only major difference was observed for high temperature NH_3 desorption peak, which followed the order Mn–SO_4^{2-}/ZrO_2–TiO_2 > SO_4^{2-}/ZrO_2–TiO_2 > Fe–SO_4^{2-}/ZrO_2–TiO_2 (refer to NH_3-TPD in Section 3.3).

3.6. Catalytic activity test

The undoped (SO_4^{2-}/ZrO_2–TiO_2), and metal doped (Fe–SO_4^{2-}/ZrO_2–TiO_2 and Mn–SO_4^{2-}/ZrO_2–TiO_2) catalysts were tested for isopropylation of benzene at benzene to isopropanol molar ratio of 10:1 and reaction temperature of 210 °C. All the reactions were performed for 5 h time on stream (TOS). It may be noted that the selection of reaction temperature and benzene to isopropanol molar ratio is not arbitrary. In our previous study [19] of this reaction over SO_4/ZrO_2–TiO_2, 100% selectivity towards alkylation products was observed when benzene to isopropanol molar ratio was 10:1 and reaction temperature 180 °C. Further, during TOS study we noticed that the deactivation of the catalyst was less at 210 °C than at 180 °C. So, to compare the activity of the above three catalysts, the best reaction conditions, as observed in our previous study [19], were maintained.

The alkylation of benzene with isopropanol is a complex reaction network. The major reaction involves alkylation of benzene with propene, formed by dehydration of isopronol, to produce cumene. But this reaction is always associated with several side reactions such as transalkylation, disproportation, dealkylation, etc., which produce a range of products. In this present case, the product stream contained cumene as the major product. The products obtained in minor quantities are 1,3 and 1,4 di-isopropylbenzene, 1,3,5 tri-isopropylbenzene and propene. It should be noted here that alkylation of benzene to cumene is often accompanied by the formation of *n*-propylbenezene and adds complexity in the separation step because of its similar physical properties with cumene. But in the present case, no *n*-propylbenze was detected in the product stream. So, based on the observations, the major reactions involved can be written as follows:

1. Isopropanol → Propene + Water
2. Benzene + Propene → Cumene
3. Cumene + Propene → Di-isopropylbenzene
4. Di-isopropylbenzene + Propene → Tri-isopropylbenzene
5. Tri-isopropylbenzene + Benzene → 2Di-isopropylbenzene
6. Di-isopropylbenzene + benzene → 2 Cumene
7. 2 Cumene → Di-isopropylbenzene + Benzene

In the present study, 100% isopropanol conversion at the end of 5 h TOS was observed for all the above three catalysts (table 2). It is worthwhile to mention that the initial step of this reaction is the dehydration of isopropanol to propene, and propene further reacts with benzene (which takes place over Bronsted acid sites) to give alkylated products. So, the total conversion of isopropanol essentially involves both dehydration and alkylation reactions. But, when conversion of benzene was considered, which reflects the alkylation activity of the catalyst, Fe–SO_4^{2-}/ZrO_2–TiO_2 showed the lowest benzene conversions among all the three catalysts (figure 5), i.e., lowest alkylation activity. With TOS, the alkylation activity went down for all of them and the effect was more prominent in case of iron doped catalyst. Further, this was clearly observed when selectivity of different product components was considered. Fe–SO_4^{2-}/ZrO_2–TiO_2 showed higher propene selectivity (51.4%) than that with SO_4^{2-}/ZrO_2–TiO_2 (15.1%), after 5 h TOS. Further, the cumene selectivity was much higher for the later case (71.8%) than former (46.1%). For Mn–SO_4^{2-}/ZrO_2–TiO_2, almost similar initial benzene conversion with respect to SO_4^{2-}/ZrO_2–TiO_2 was

Table 2
Effect of metal ion doping on isopropylation activity and selectivity of different products over undoped and Fe and Mn doped SO_4^{2-}/ZrO_2–TiO_2 mixed oxide catalysts calcined at 600 °C

	Catalyst					
	SO_4^{2-}/ZrO_2–TiO_2(S)		Fe–SO_4^{2-}/ZrO_2–TiO_2		Mn–SO_4^{2-}/ZrO_2–TiO_2	
Reaction time	1 h	5 h TOS	1 h	5 h TOS	1 h	5 h TOS
Isopropanol conversion, %	100	100	100	100	100	100
Benzene conversion, %	10.38	8.37	6.56	5.63	10.34	9.8
#Benzene conversion, %	10.3	8.2	–	–	10.3	9.6
Coke content, g	–	1.76	–	1.1	–	1.14
Selectivity of different products, mol%						
Cumene	97.1	71.8	65.7	46.1	92.4	72.3
1,3 DIPB	2.1	7.5	2.6	0.3	6.1	5.6
1,4 DIPB	0.8	5.6	4.3	2.0	1.5	2.8
1,3,5 TIPB	–	Trace	0.8	0.2	Trace	1.4
Propene	–	15.1	26.6	51.4	–	17.9

Note: Reaction temperature = 210 °C, WHSV = 3.65 h^{-1}, benzene:isopropanol = 10:1(mol/mol).
#Benzene conversion of the 550 °C regenerated catalyst (air, 3 h).

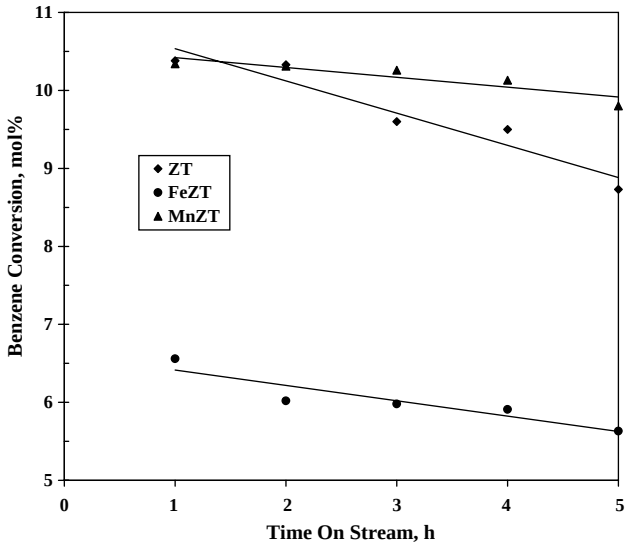

Figure 5. Effect of metal doping on benzene alkylation activity as a function of TOS over undoped, and iron and manganese doped SO_4^{2-}/ZrO_2–TiO_2 mixed oxide catalysts calcined at 600 °C.

observed (10.34% against 10.38 for SO_4^{2-}/ZrO_2–TiO_2, figure 5 and table 2), which indicates similar initial alkylation activity. As far as selectivity of cumene is concerned, the undoped catalyst showed higher initial cumene selectivity than that of the Mn-doped catalyst. But, after 5 h TOS, the benzene conversion for Mn doped catalyst was much higher than that for undoped catalyst, which indicates higher alkylation activity for Mn doped catalyst and higher stability under these reaction conditions. Also, it showed slightly higher cumene selectivity. But, as far as selectivity towards di- and tri-isopropylbenzenes are concerned, the Mn promoted catalyst showed lower di-isopropylbenzene (DIPB) and higher tri-isopropylbenzene selectivity. This shows the further alkylation of primary alkylation products, which is either due to presence of stronger acidic sites or strong adsorption of primary products on the Mn–SO_4^{2-}/ZrO_2–TiO_2 surface. From the ^{1}H MAS NMR results it was observed that the Mn doped catalyst contained surface protons of highest acid strength and the Fe doped catalyst lowest. Further, from TPR analysis it was observed that the enhancement of acidity was due to the stabilization of surface sulfate groups upon Mn doping. So, this enhancement of isopropylation activity for Mn doped catalyst could be attributed to the increased protonic acid strength through stabilization of surface sulfate groups. Furthermore, the isopropylation activity followed the order Mn–SO_4^{2-}/ZrO_2–TiO_2 > SO_4^{2-}/ZrO_2–TiO_2 > Fe–SO_4^{2-}/ZrO_2–TiO_2, which is, in fact, the same as that of the acidity order determined by ^{1}H MAS NMR.

Most of the earlier reports have proposed that deactivation of the catalyst during alkylation is because of the coke deposition on the active sites [31,32]. Further, the coke formation depends upon the operating conditions as well as characteristics of the material such as acidity, pore structure, etc. The origin of coke molecules on the surface of zeolitic catalysts involved in cumene synthesis reaction depends mainly upon two factors; low volatility or steric blocking. In general, retention of coke molecules related to the low volatility dominates at low temperature, whereas that due to trapping of higher molecular weight bulky molecules (sterically blocked) occurs at high temperature [33]. Also, it has been accepted that higher the acidity of the catalyst greater will be the coke formation [33]. Therefore, attempt was made to find out the possible cause of deactivation.

As discussed earlier all catalysts deactivate with TOS (table 2); but the least deactivation, i.e., the highest benzene conversion after 5 h TOS, was observed in case of Mn–SO_4^{2-}/ZrO_2–TiO_2. The spent catalysts (undoped

and Mn doped) were regenerated at 550 °C for 3 h under air flow (30 mL/min) and the same reaction was performed. Both of them regained their activity (table 2, raw-5). So, the carbon contents of all the spent catalysts were measured by a CHN analyzer and the results are presented in table 2 (raw-6). Mn doped catalysts showed less coke content than the undoped catalyst. Although, the Fe doped catalyst contained the lowest amount of coke, its initial alkylation activity was much less than the undoped and Mn doped catalysts, possibly due to its less acidity as discussed in case on NH_3-TPD and ^1H MAS NMR results. On the other hand, the Mn doped catalyst contained lower amounts of coke than the undoped catalyst, even though its acidity was higher and so also its activity. It can be said that coking is the possible cause of deactivation in this case. When the catalysts were regenerated in presence of air at 550 °C, the coke deposited over active sites were burnt off and the shielded active sites were again exposed to interact with the reactant molecules.

4. Conclusions

^1H MAS NMR results indicated that the protonic acid strength of this catalyst was increased when SO_4^{2-}/ZrO_2–TiO_2 was doped with Mn. On the other hand, protonic acid strength decreased upon doping with Fe, and the acidity of the three catalysts followed Mn–SO_4^{2-}/ZrO_2–TiO_2 > SO_4^{2-}/ZrO_2–TiO_2 > Fe–SO_4^{2-}/ZrO_2–TiO_2. The same result was further supported by TPD analysis in which the high temperature NH_3 desorption peak was observed at the highest temperature, upon doping with Mn. The acidity measurements in conjunction with the TPR analysis confirmed that the increase in acidity in case of Mn doped catalyst was due to the enhanced stabilization of surface sulfate groups. The activity towards isopropylation of benzene was also highest for Mn doped catalyst and followed the same order as their acidity. This catalyst showed highest activity with the lowest deactivation after 5 h TOS. This was attributed to the increase in protonic acid strengths through stabilization of surface sulfate species. The decrease in activity of the catalysts was due to the coke formation over the active sites.

Acknowledgments

The financial support to Dr. A.K. Dalai as part of the Canada Research Chair program is highly acknowledged. The authors acknowledge Dr. N.C. Pradhan for his suggestions and valuable discussions. Thanks are also due to B. Chatson, NRC, Saskatoon, Canada, for his help in carrying out ^1H MAS NMR analysis.

References

[1] M. Hino and K. Arata, J. Chem. Soc. Chem. Commun. (1980) 851.
[2] T. Yamaguchi, T. Jin and K. Tanabe, J. Phys. Chem. 90 (1986) 3148.
[3] K. Arata and M. Hino, Mater. Chem. Phys. 26 (1990) 213.
[4] T. Yamaguchi, Appl. Catal. A: Gen. 61 (1990) 1.
[5] K. Arata, Adv. Catal. 37 (1990) 165.
[6] E. Iglesia, S.L. Soled and G.M. Kramer, J. Catal. 144 (1993) 238.
[7] M.Y. Wen, I. Wender and J.W. Tierney, Eng. Fuels 4 (1990) 372.
[8] T. Hosai, T. Shimadzu, S. Itoh, S. Baba, H. Takaoka, T. Imai and M. Yokoyama, Prepr. Am. Chem. Soc. Div. Petr. Chem. 33 (1998) 562.
[9] A. Sayari and A. Dicko, J. Catal. 145 (1995) 561.
[10] C.-Y. Hsu, C.R. Heimbuch, C.T. Armes and B.C. Gates, J. Chem. Soc. Chem. Commun. (1992) 1645.
[11] M.S. Scurrel, Appl. Catal. A: Gen. 34 (1987) 109.
[12] K. Tanabe, T. Sumiyoshi, K. Shibata, T. Kiyoura and J. Kitagawa, Bull. Chem. Soc. Jpn. 47 (1974) 1064.
[13] D. Das, H.K. Mishra, K.M. Parida and A.K. Dalai, J. Mol. Catal. A: Chem. 189 (2002) 271.
[14] K. Arata, S. Akutagawa and K. Tanabe, Bull. Chem. Soc. Jpn. 49 (1976) 390.
[15] I. Wang, W.F. Chang, R.J. Shiau, J.C. Wu and C.S. Chung, J. Catal. 83 (1983) 428.
[16] Y. Hirashima, K. Nishiwaki, A. Miyakoshi, S. Tsuiki, V. Ueno and H. Nakabayashi, Bull. Chem. Soc. Jpn. 61 (1988) 1945.
[17] J. Fung and I. Wang, J. Catal. 130 (1991) 577.
[18] K. Hashimoto, T. Masuda and H. Kashihara, Appl. Catal. A: Gen. 75 (1991) 331.
[19] D. Das, H.K. Mishra, A.K. Dalai and K.M. Parida, Appl. Catal. A: Gen. 243(2) (2003) 271.
[20] R. Barthos, F. Lonyi, G.Y. Onyestyak and J. Valyon, Solid State Ionics 141 (2001) 253.
[21] R. Barthos, F. Lonyi, G.Y. Onyestyak and J. Valyon, J. Phys. Chem. B 104 (2000) 7311.
[22] D. Freude, M. Hunger and H. Pfeifer, Z. Phys. Chem. (Frankfurt) 152 (1987) 171.
[23] V.M. Mastikhin, I.L. Mudrakovsky and A.V. Nosov, Prog. Nucl. Mang. Reson. Spectrosc. 23 (1991) 259.
[24] U. Fleischer, W. Kutzelnigg, A. Bleicher and J. Sauer, J. Am. Chem. Soc. 115 (1993) 7833.
[25] T. Reimer, D. Spielbauer, M. Hunger, G.A.H. Mekhemer and H. Knozinger, J. Chem. Soc. Chem. Commun. (1994) 1181.
[26] V. Semmer, P. Batamack, C.D. Morin, R. Vincent and J. Fraissard, J. Catal. 161 (1996) 186.
[27] B.-Q. Xu and W.M.H. Sachtler, J. Catal. 167 (1997) 224.
[28] K. Ebitani, T. Tanaka and H. Hattori, Appl. Catal. A: Gen. 102(2) (1993) 79.
[29] A. Dicko, X. Song, A. Adnot and A. Sayari, J. Catal. 150 (1994) 254.
[30] R. Srinivasan, R.A. Keogh, D.R. Milburn and B.H. Davis, J. Catal. 153 (1995) 123.
[31] J. Panming, W. Qiuying, Z. Chao and X. Yanhe, Appl. Catal. A: Gen. 91 (1992) 125.
[32] A. Corma, V.M. Soria and E. Schoeveld, J. Catal. 192 (2000) 163.
[33] M. Guisnet and P. Magnoux, in: *Zeolite Microporous Solids*: *Synthesis*, *Structure and Reactivity* eds. E.G. Derouane, F. Limos, C. Naccache and F.R. Ribeiro, NATO ASI series C, 352 (Kluwer, Dordrecht, 1992) 437 pp.